PAPER
A Row-Parallel Position Detector for High-Speed 3-D Camera Based on Light-Section Method

Yusuke OIKE[†a)], *Student Member*, Makoto IKEDA[†], *and* Kunihiro ASADA[†], *Regular Members*

SUMMARY   A high-speed 3-D camera has a future possibility of wide variety of application fields such as quick inspection of industrial components, observation of motion/destruction of a target object, and fast collision prevention. In this paper, a row-parallel position detector for a high-speed 3-D camera based on a light-section method is presented. In our row-parallel search method, the positions of activated pixels are quickly detected by a row-parallel search circuit in pixel and a row-parallel address acquisition of $O(\log N)$ cycles in N-pixel horizontal resolution. The architecture keeps high-speed position detection in high pixel resolution. We have designed and fabricated the prototype position sensor with a 128×16 pixel array in $0.35\,\mu\mathrm{m}$ CMOS process. The measurement results show it achieves quick activated-position acquisition of $450\,\mathrm{ns}$ for "beyond-real-time" 3-D imaging and visual feedback. The high-speed position detection of the scanning sheet beam is demonstrated.
key words: position detector, smart image sensor, high speed, row-parallel architecture, 3-D camera

1. Introduction

A high-speed 3-D camera has a future possibility of wide variety of application fields such as quick inspection of industrial components, observation of motion/destruction of a target object, and fast collision prevention. Some range finding methods were proposed for range finding such as a light-section method, a stereo-matching method and a time-of-flight method. In the typical methods, a light-section method can achieve higher range accuracy with simple calculation in general. Both high range accuracy and simple calculation are important for the applications of a high-speed 3-D camera. A high-speed 3-D camera requires high-speed beam scanning, strong beam intensity, quick position detection, high-speed data transmission and high-speed range calculation. Now we can have a high-speed scanning mirror and a strong laser beam source to realize 1000 range_maps/sec though it depends on applications. And then the range calculation of a light-section method is simple because it has no block matching such as a stereo-matching method. In 2-D imaging, some high-speed image sensors with 500–10k fps [1], [2] were presented to capture a fast-moving object. High-speed 3-D imaging based on a light-section method,
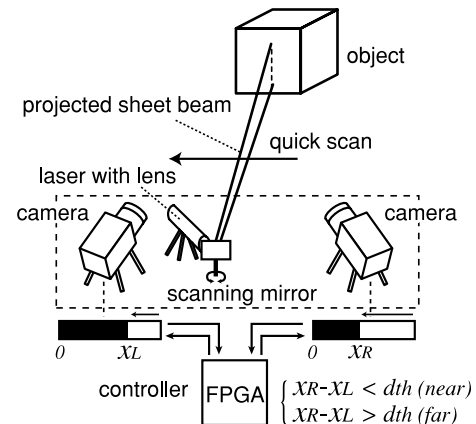
Fig. 1   An example of high-speed range detection system.

however, requires much higher speed of frame rate than high-speed 2-D imaging since an image sensor must detect a lot of positions of a scanning beam on the sensor plane to get a range map. Moreover it is difficult to transfer data of full images captured by a standard imager in higher frame rate for fast range finding. Therefore it is important to achieve high-speed position detection and to provide only efficient information for range finding to reduce data transmission.

For example, Fig. 1 shows a high-speed range detection system. The scanning sheet beam activates pixels from the right to the left on the sensor plane. Then two position sensors detect the edge of activated pixels. The difference between x_R and x_L represents the distance from the position sensors. Here the edge address of the left position sensor is x_L and that of the right one is x_R. One scan with N-pixel horizontal resolution requires N frames of the scanning sheet beam. That is, to realize 30 range_maps/sec 3-D imaging with 1k-pixel horizontal resolution, an image sensor must operate 1000 position detections of projected beam during one beam scanning. In other words, it requires 30k-fps position detection rate, and quick position detection realizes a high-speed and high-resolution 3-D camera. Therefore some smart sensors [3]–[8] were proposed for high-speed position detection of a scanning laser beam in range finding based on a light-section method.

The smart sensors [5]–[8] are useful for high-speed position detection. Since a high-speed 3-D camera with 1k range_maps/sec requires 1M-fps position detection

rate, the frame rates of these sensors are not enough to realize a high-speed 3-D camera for real-time or more high-speed range finding with high pixel resolution. Though some of the smart sensors have a capability of high-speed position detection rate using LEP (Lateral Effect Photodiode) [5], it is difficult to be applied to a scene with non-uniform background illumination and/or a target object with a rough surface. In addition, it requires high accurate ADCs to realize high resolution. A 64×32 position sensor using a current-mode WTA (Winner-Take-All) circuit [6] achieves 6.4k fps. The pixel resolution is, however, limited by the precision of the current-mode WTA circuit. It is also difficult to realize high frame rate enough for real-time 3-D measurement in high pixel resolution. A color image sensor with a 320×240 pixel array [8] has been presented to avoid some problems of their previous work [7]. It realizes 3.3k fps in 160×120 resolution due to reducing a pixel circuit and its power dissipation. Its frame rate is the outer limit for real-time 3-D measurement in 160×120 pixels.

In this paper, a row-parallel position detector for a high-speed 3-D camera based on a light-section method is presented. In our row-parallel search architecture, the positions of activated pixels are quickly detected by a row-parallel search circuit in pixel and a row-parallel address acquisition of $O(\log N)$ cycles in N-pixel horizontal resolution. It has the capability of high frame rate for real-time or more high-speed range finding with high pixel resolution. We have designed and successfully tested the prototype position detector with a 128×16 pixel array in $0.35\,\mu$m CMOS process and also evaluated the performance of the prototype chip.

2. Principle of Range Finding Based on Light-Section Method with 2 Cameras

To get range data using simple calculation, we have focused on a range finding system based on a laser range finder with 2 cameras as shown in Fig. 1. The light-section system usually use a pair of one laser scanner and one sensor since the range data can be acquired by them using a triangulation principle. It requires accurate swing control of beam scanning for triangulation, however it becomes difficult for a high-seed 3-D imaging system since the scanning speed becomes very faster. Therefore the high-speed 3-D system requires two position sensors for triangulation with rough beam scanning. The system provides range data based on triangulation using the positions of the projected light on each sensor plane. Differently from a 1-camera/1-laser system, it does not require precise control of a scanning laser beam. Therefore it allows high-speed laser beam scanning and realizes fast range detection in proportion to frame rate of a position detector because of simple calculation. Figure 2 shows a principle of triangulation-based range finding for a high-speed 3-D camera. Two
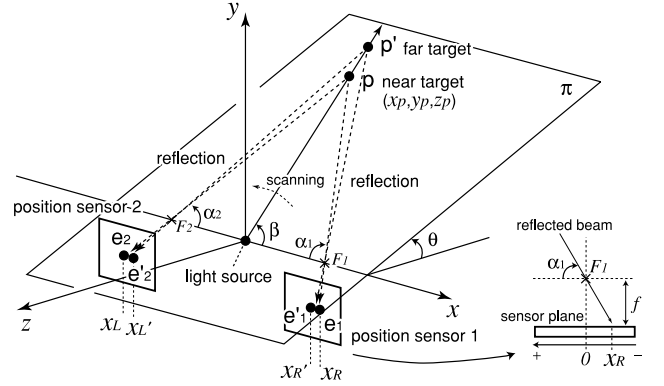

Fig. 2 Principle of triangulation-based range finding for high-speed 3-D camera.

position sensors detect the position of the beam reflection respectively. For example, the right position sensor detects it as e_1 at $x = x_R$ and the left one detects it as e_2 at $x = x_L$ when a target object is placed at $p(x_p, y_p, z_p)$. α_1 and α_2 can be calculated using the detected positions x_R and x_L from each position sensor as follows:

$$\tan \alpha_1 = -\frac{f}{x_R} \tag{1}$$

$$\tan \alpha_2 = \frac{f}{x_L} \tag{2}$$

where f is a focal depth of cameras. α_1 and α_2 are also represented by

$$\tan \alpha_1 = \frac{l}{d/2 - x_p} \tag{3}$$

$$\tan \alpha_2 = \frac{l}{d/2 + x_p} \tag{4}$$

where d is a distance between two position sensors and l is length of a perpendicular line from p to x-axis. Therefore x_p and l are given by

$$x_p = \frac{d(\tan \alpha_1 - \tan \alpha_2)}{2(\tan \alpha_1 + \tan \alpha_2)} \tag{5}$$

$$l = \frac{d \tan \alpha_1 \tan \alpha_2}{\tan \alpha_1 + \tan \alpha_2} \tag{6}$$

Here $y_p = l \sin \theta$ and $z_p = -l \cos \theta$ where θ is a field angle of camera view decided by y-address of the detected position on the sensor plane.

$$y_p = \frac{d \tan \alpha_1 \tan \alpha_2 \sin \theta}{\tan \alpha_1 + \tan \alpha_2} \tag{7}$$

$$z_p = -\frac{d \tan \alpha_1 \tan \alpha_2 \cos \theta}{\tan \alpha_1 + \tan \alpha_2} \tag{8}$$

From Eq. (1) and Eq. (2), $x_R - x_L$ is given by

$$x_R - x_L = -\frac{f(\tan \alpha_1 + \tan \alpha_2)}{\tan \alpha_1 \tan \alpha_2} \tag{9}$$

Compared between Eq. (8) and Eq. (9), we have

$$z_p = \frac{f \cdot d \cos \theta}{x_R - x_L} \qquad (10)$$

The accurate range data are acquired as described above.

Rough range data can be calculated more simply for some applications of quick range detection such as collision prevention. From Eq. (10), $|z_p|$ is a monotone increasing function in terms of $x_R - x_L$ as follows:

$$|z_p| \propto -\frac{1}{x_R - x_L} \qquad (11)$$

Therefore the difference between two addresses represents the distance from the sensors to a target object. Thus in such a situation as collision prevention, we define a threshold level d_{th} for range detection and we can quickly know if an object is placed within z_{th} or not as follows:

$$x_R - x_L < d_{th} \quad (near) \qquad (12)$$
$$x_R - x_L > d_{th} \quad (far) \qquad (13)$$

where we assume a target field angle of y-axis is narrow and then $\cos \theta = 1$. A range threshold z_{th} for collision prevention is given by

$$z_{th} = \frac{d \cdot f}{d_{th}} \qquad (14)$$

In such a system, it is important to detect the position of a high-speed scanning beam and provide its position address quickly.

3. Row-Parallel Architecture

In the position detection of a projected sheet beam, a sensor recognizes the pixels with strong incident intensity as the history of the scanning sheet beam as shown in Fig. 3. Therefore it is important to quickly detect the position of the activated pixels in each row. The frontier line of the projected light provides enough information for triangulation-based range finding. Our
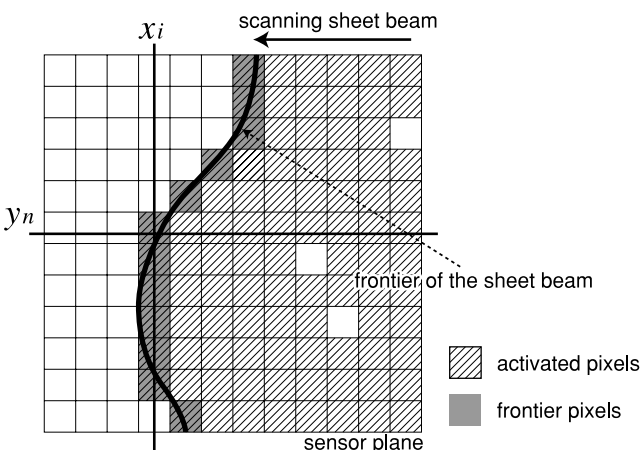
sensor architecture has a pixel array with in-pixel and row-parallel search circuits for activated pixels, a row-parallel address acquisition of $O(\log N)$ cycles in N-pixel horizontal resolution, and a row-parallel processor to reduce data transmission as shown in Fig. 4. Figure 5 shows flow charts of activated pixel detection. When we use a standard binary image sensor with $N \times M$ pixel resolution, M-times access for every row line is needed to get the position of projected sheet beam as shown in Fig. 5(a). On the other hand, our architecture requires no iteration due to the row-parallel position detection and address acquisition as shown in Fig. 5(b).

3.1 Pixel Circuit for Row-Parallel Search

Figure 6 shows a schematic of a pixel. It has a photodiode with a reset transistor, a threshold logic and latch circuit, a search circuit, and an address acquisition circuit. The voltage of a floating node at a photo diode decreases according to incident light intensity after reset. It is digitized by a threshold logic and the result is latched. V_{rst} is a reset voltage and it enables to change the threshold margin. The pixel activation rate becomes faster when the reset voltage V_{rst} is set to lower. It is limited by S/N caused by fluctuation of the threshold level and a non-uniform ambient incident light. The latch circuit can invert a pixel value PIX using an XOR circuit. At the search circuit, the
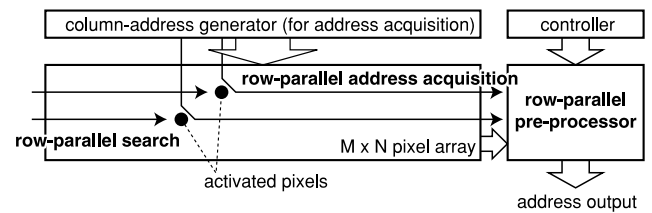

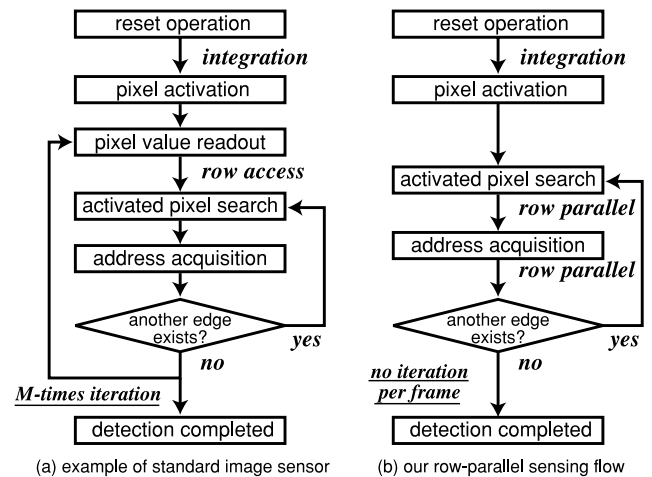**Fig. 4** Block diagram of our sensor architecture.

(a) example of standard image sensor   (b) our row-parallel sensing flow

Fig. 5 Flow charts of activated pixel detection: (a) an example of a standard binary image sensor, (b) our row-parallel architecture.

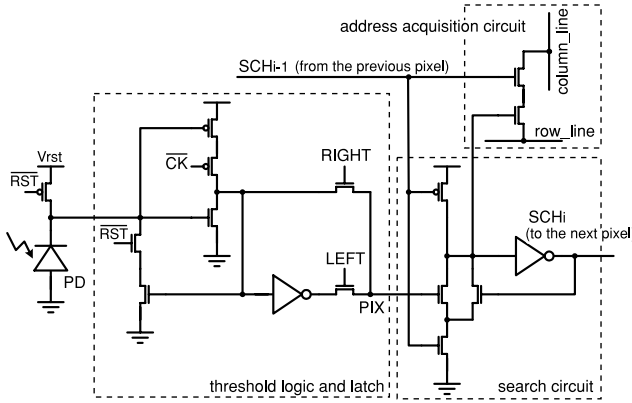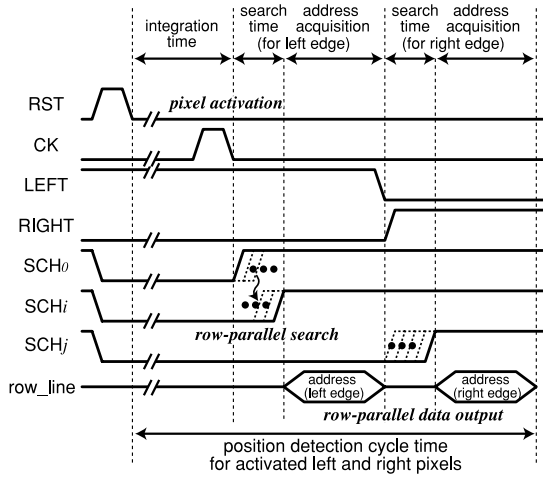**Fig. 3** Captured image example of a sheet beam.

Fig. 6 Pixel circuit.

Fig. 7 Timing diagram of activated pixel detection.

Fig. 8 Procedure of row-parallel position search.

passes through activated pixels with strong incident intensity and stops again at the first-detected pixel without strong incident intensity, which is the next pixel of the activated right edge x_j. If only the frontier position of the scanning beam is required, a frame readout operation is completed at the first search period. The next search period using inverted pixel values provides the activated right edge to get the center position of the projected beam. In addition, the positions of the second and more activated pixels are detectable by the iteration of PIX inversions. It means that it is applicable to applications with a complex-shaped target object and multiple projected lights. The timing diagram of the activated pixel detection is shown in Fig. 7.

3.2 Row-Parallel Address Acquisition

The address acquisition circuit of the pixel circuit consists of only 2 pass transistors as shown in Fig. 6. At the detected pixel of each row, the column line is connected to the row line via the pass transistors as shown in Fig. 9. Then, the serial-bit-streamed column address is applied to each column line in parallel. Only the address of the detected pixel runs into each row line through the pass transistors. In each row, a row-parallel preprocessor receives the serial-bit-streamed address of the detected pixel. Therefore the address acquisition cycles are $O(\log N)$ in N-pixel horizontal resolution. The compact in-pixel circuit implementation and the high-speed row-parallel address acquisition contribute quick position detection in high pixel resolution.

3.3 Row-Parallel Processor

The position sensor has row-parallel processors as shown in Fig. 10. Each consists of a latch sense amplifier to get the address data, a full adder, random access memories with a read/write circuit, output buffers for

search signal SCH_{i-1} from the previous pixel passes to the next pixel when PIX is '1.' On the other hand, it stops when PIX is '0.' That is, it stops at the first-detected pixel with strong incident intensity. The address of the detected pixel is acquired in row parallel using two pass transistors as described in Sect. 3.2. The present pixel circuit utilizes dynamic circuit techniques to reduce the number of transistors in pixel. Therefore it has a possible problem of noise immunity when the pixel resolution becomes higher, so it should be implemented by static circuits for very large pixel resolution in the future.

Figure 8 shows a procedure of the row-parallel search for activated pixels. Some pixels are activated by strong incident intensity and they have a pixel value PIX of '0' as shown in Fig. 8(a). The search signal SCH_0 is provided to each row at the left pixels (x_0, y_n). It passes to the next pixel when the pixel value PIX is '1.' Thus the search signal stops at the left edge x_i of the activated pixels as shown in Fig. 8(b). After a row-parallel address acquisition mentioned later, the pixel values are inverted using in-pixel XOR circuit and the search signal starts again. In this period, it
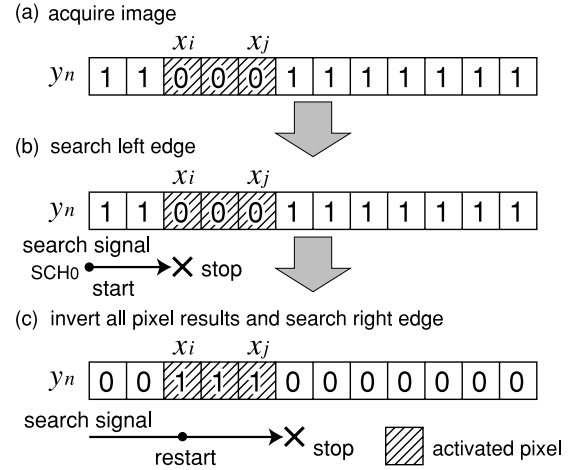
a) Address acquisition for the left edge

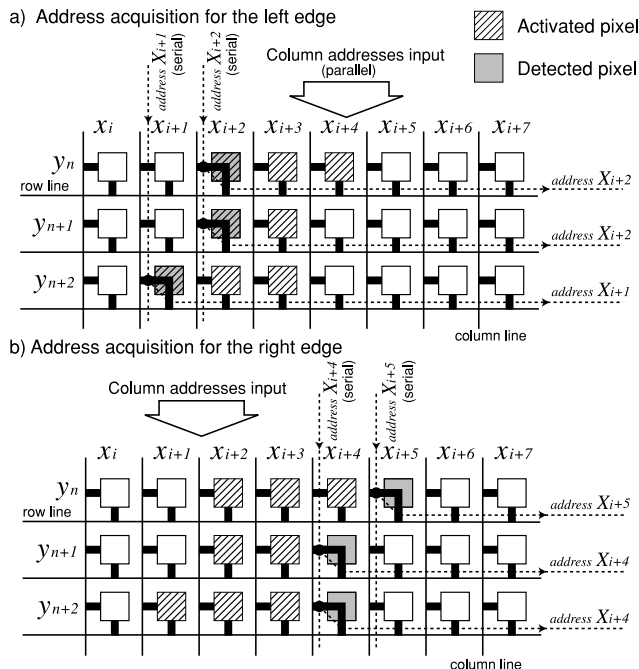b) Address acquisition for the right edge

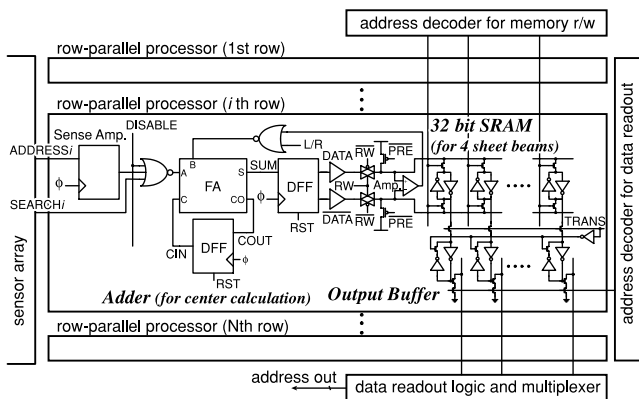**Fig. 9**   Method of row-parallel address acquisition.

Fig. 10   Structure of row-parallel processor.

pipe-lined data readout, and some control logics. It receives the bit-serial-streamed addresses of x_i and $x_j + 1$ in row-parallel address acquisition when the left and right activated pixels with strong incident intensity are at x_i and x_j. A latch sense amplifier holds the bit-serial address of x_i and stores it to 32-bit SRAM if the search signal does not arrived, that is, an activated pixel still exists in the row. On the other hand, the address 0 is stored in the SRAM of a row without activated pixels. It is interpreted as no activated pixel in post handling. When the frontier position of the scanning laser beam is needed, the address data in SRAM are transferred to output buffers and read out. To get the center position of the activated pixels in a 1-camera/1-laser system, the next bit-serial address of $x_j + 1$ is accumulated on the left-edge address x_i in row parallel before transferred and read out. The 32-bit SRAM has the capability of
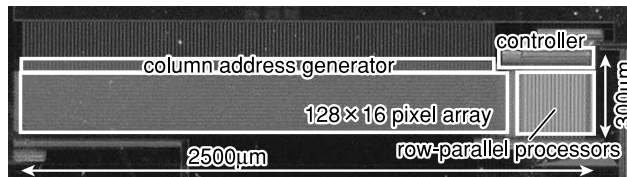

Fig. 11   Chip microphotograph.

Table 1   Specifications of the prototype chip.

Process	$0.35\,\mu$m CMOS 3-metal 1-poly-Si
Sensor size	$2.5\,$mm $\times\ 0.3\,$mm
# pixels	128×16 pixels
Pixel size	$16.25\,\mu$m $\times\ 16.25\,\mu$m
# trans. / pixel	18 transistors
Fill factor	20.15 %

four edge addresses of activated pixels or four accumulated addresses of left and right activated edges. The preprocessing contributes to reduce data transmission. And also it realizes to get the positions of multiple sheet beams in one frame.

The row-parallel processor can be extended to deal with another data processing. For example, multiple samplings per frame can be realized to get an intensity profile information of a projected beam for high sub-pixel accuracy when a timing memory and its control logics are implemented. It will contribute to improve range accuracy of 3-D shape measurement.

4.   Chip Implementation

We have designed and fabricated a prototype position sensor in $0.35\,\mu$m CMOS process. Figure 11 shows a microphotograph of the fabricated chip. It consists of a 128×16 pixel array, a column address generator, row-parallel processors with 32 bit SRAM per row and a memory controller. The pixel circuit has 1 photo diode and 18 transistors in $16.25\,\mu$m $\times\ 16.25\,\mu$m pixel area with 20.15 % fill factor. The position sensor occupies $2.5\,$mm $\times\ 0.3\,$mm area. The specifications of the prototype chip are shown in Table 1.

5.   Performance Evaluation

5.1   Limiting Factors of Frame Rate

Range finding based on a light-section method can be realized by two ways of position detection, a reset-per-scan mode and a reset-per-frame mode. The pixels with high integration level by incident intensity are activated in the position detection modes.

In a reset-per-scan mode, the integration time of each pixel takes one scan interval after reset operation. The activated frontier positions of the scanning beam are detected during the integration. Here the limiting factors of frame rate are the access rate of activated pixels and the incident intensity of scanning beam. The
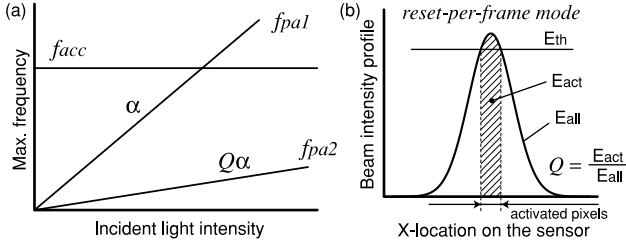
Fig. 12 Limiting factors of frame rate in reset-per-frame mode and reset-per-scan mode.

frame rate f_{psd} are given by

$$f_{psd} = \frac{1}{\max(T_{acc}, T_{pa1})} = \min(f_{acc}, f_{pa1}) \qquad (15)$$

where T_{acc} and f_{acc} are the access time and rate of activated pixels, and T_{pa1} and f_{pa1} are the pixel-activation time and rate with scanning beam as shown in Fig. 12(a). The access rate f_{acc} is decided by the search time for activated pixels. The pixel-activation rate f_{pa1} is associated with the integration time to exceed a threshold level after reset, and decided by the intensity of the scanning beam. The reset-per-scan mode has a possibility of high frame rate by short access interval though it needs plenty strong incident intensity of a projected beam against ambient illumination. But then this mode is not applicable to some specific cases with complex shaped and multiple target objects since we assume the projected beam is scanned in one direction from the left to the right on the sensor plane.

In a reset-per-frame mode, the integration time takes one frame interval with reset operation. The operation of position detection is carried out after the integration with reset operation. Thus the frame interval is the total of integration time and access time for activated pixels. The frame rate f_{psd} is given by

$$f_{psd} = \frac{1}{T_{acc} + T_{pa2}} = \frac{f_{acc} \cdot f_{pa2}}{f_{acc} + f_{pa2}} \qquad (16)$$

where T_{pa2} and f_{pa2} are the pixel-activation time and rate with scanning beam in a reset-per-frame mode as shown in Fig. 12(a). The pixel-activation rate f_{pa2} is decided by the intensity of the scanning beam in the same way as f_{pa1}. The sensitivity of the reset-per-frame mode is, however, lower than that of the reset-per-scan mode since the projected beam has intensity profile with spatial distribution as shown in Fig. 12(b). The intensity of non-activated pixels, which is under the threshold level E_{th}, are wasted by reset operation in the next frame of the reset-per-frame mode. The efficiency Q of incident intensity is given by

$$Q = \frac{E_{act}}{E_{all}} \qquad (17)$$

where E_{all} is the total intensity of the projected beam and E_{act} is the total intensity at activated pixels.
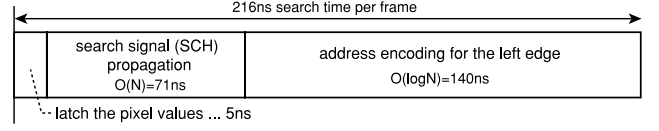

Fig. 13 Simulated search time per frame for position detection of the fabricated chip.
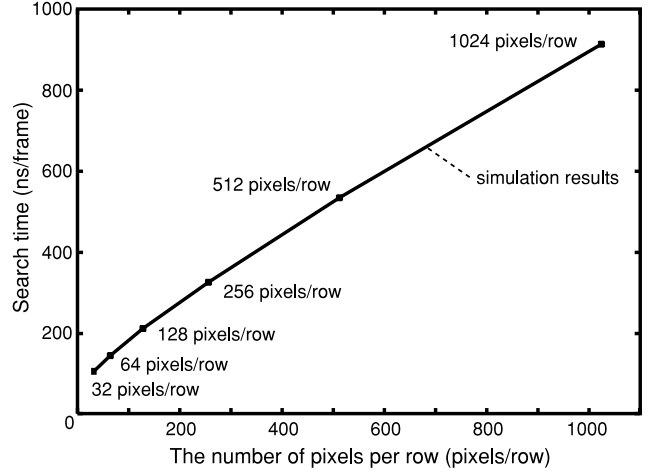

Fig. 14 Simulated search time in high pixel resolution.

Therefore the pixel-activation rate of the reset-per-frame mode is lower than that of the reset-per-scan mode in the same situation as shown in Fig. 12(a). High-speed access rate f_{acc} makes frame rate faster though f_{pa2} is dominant in the situation without sufficient beam intensity. Differently from the reset-per-scan mode, the reset-per-frame mode can be applied to complex shaped and multiple target objects since the behavior of projected beam on the sensor plane is unrestricted due to reset operation per frame.

5.2 Access Rate and Pixel Resolution

Figure 13 shows search time per frame for position detection simulated by HSPICE. The maximum propagation delay of the search signal is 71 ns and the 7-bit address acquisition for 128 columns takes 140 ns. The total search time to get the position of the left activated edge is 216 ns per frame.

In a reset-per-frame mode, the frame interval, the total of the integration time of incident light and the search time for activated pixels, is $30.2\,\mu s$ where we assume the integration time of incident light is $30\,\mu s$. In a reset-per-scan mode, the search operation is iterated and the frontier positions of the scanning sheet beam is detected during photo current integration. The frame interval is the same as the search time if we have plenty strong intensity of scanning beam. Figure 14 shows the relationship between the row-pixel resolution and the search time of activated pixel. Here we assume that the column-pixel resolution is the same as the row-pixel

resolution (i.e. $N \times N$ pixel resolution) and the activated pixels are laid in the same vertical line because it is the worst case due to capacitive load of address lines. Generally real-time range finding (30 range_maps/sec) with 1024×1024 pixels requires $32.5\,\mu s$ search time. The present architecture achieves $918\,ns$ search time per frame at 1024-pixel horizontal resolution in $0.35\,\mu m$ CMOS process as shown in Fig. 14. It realizes enough speed for not only real-time but also beyond-real-time range finding and visual feedback.

5.3 Sub-Pixel Accuracy of Position Detection

Range accuracy based on a light-section method is decided by many factors such as a position detection scheme, pixel resolution, scanning mirror accuracy, a optical setup, parallax of a measurement system and so on. The factors except for sensor characteristics are common among our sensor and the conventional sensors [6], [8]. And the range resolution is proportion to the column-pixel resolution. Therefore we focus on the sub-pixel accuracy for accuracy comparison among the conventional detection schemes. Almost all conventional high-speed sensors get the pixels over the threshold level to detect the position of projected beam. That is, their position detection is based on a binary image as well as our sensor. Therefore the sub-pixel accuracy is about 0.5 sub-pixel accuracy due to center calculation. For example, the sub-pixel resolution of the sensor [6] corresponds to 64×64 pixels though it has just 64×32 pixel resolution. On the other hand, the sensor [8] has a kind of timing memories and its range accuracy depends on the frame rate. Its frame rate is 3.3k fps with 160 column-pixel resolution and the beam-scanning rate is 15 Hz. It corresponds to 220 lines per range map. In this case, the sub-pixel accuracy of [8] is 0.72 pixels. Our row-parallel architecture achieves 0.5 and 1.0 sub-pixel accuracy in a reset-per-frame mode and a reset-per-scan mode respectively since the reset-per-frame mode allows center calculation using the left- and right-edge positions and the reset-per-scan mode detects only the frontier position without center calculation.

All of these sensors recognize a pixel over the threshold level as an activated pixel. Therefore they have a possibility of activation error by the threshold level fluctuation. Their threshold levels have some margin and the projected beam has sharpen edges in general, so the activation error is caused at the edges of the incident beam. Therefore the activation error corresponds to 0.5 sub-pixel resolution in maximum.

6. Measurement Results and Discussion

The measurement system of the fabricated chip has been developed as shown in Fig. 15. It consists of the fabricated position detector on a test board, a scanning
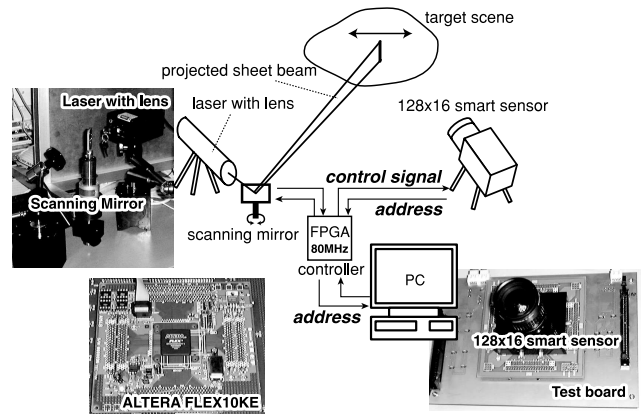

Fig. 15 Measurement system.

mirror with $300\,mW$ laser beam source ($665\,nm$ wavelength), an FPGA for system control, and a host PC. In the system, the position detector and a scanning mirror are controlled by the FPGA and the acquired position data are transferred to a host PC after capturing. The FPGA was operated at $80\,MHz$ due to the limitation of the testing equipment. In this case, the search time was $450\,ns$ per frame and the integration time of incident light was $30\,\mu s$ at $V_{rst} = 1.4\,V$. The search time is limited by control speed of the FPGA in the measurement. To realize a 2-camera system for a high-speed 3-D imaging, the hardware cost becomes double for control of two position sensors. The computational effort of range calculation is almost the same since just the detected positions of the additonal sensor is used for triangulation instead of the swing position of scanning mirror. The data transmission, however, becomes double if the range calculation is not carried out on the FPGA.

Figure 16 shows the measurement results of the present position detector. The acquired position of the left and right activated pixels was acquired as shown in Fig. 16(a). That is, the projected sheet beam is located between these edges on the sensor plane. The position detector has a row-parallel processor to calculate the center position on the chip to reduce data transmission.

Figure 16(b) shows sequentially captured positions of the scanning sheet beam of $2\,kHz$ by a reset-per-frame mode. Here the position detector provides the center address calculated by the row-parallel processor. The measurement result shows that the access rate of activated pixels f_{acc} is $2.22\,MHz$ and the pixel-activation rate f_{pa2} is $33.3\,kHz$. In the measurement, the center position of a projected beam is calculated on the sensor plane, so two search operations for the left and right activated pixels are needed. 256 effective pixel resolution is realized by the center calculation to improve range accuracy. Here the frame interval takes $30.9\,\mu s$ per frame (f_{psd}=32.2k fps), which includes $30.0\,\mu s$ integration time.

Figure 16(c) shows the frontier positions of the scanning sheet beam during integration in a reset-per-scan mode. In the measurement situation, 2 kHz mirror scanning within the camera angle is limited by a scan drive of galvanometer mirror. Though the frame interval of $4\,\mu s$ is sufficient to get the position of 2 kHz scanning beam, this sensor achieves up to 2.22M fps as the same as the access rate f_{acc}. In this regard, the scan speed requires 17.4 kHz to get full performance of the position sensor with 128-pixel horizontal resolu-
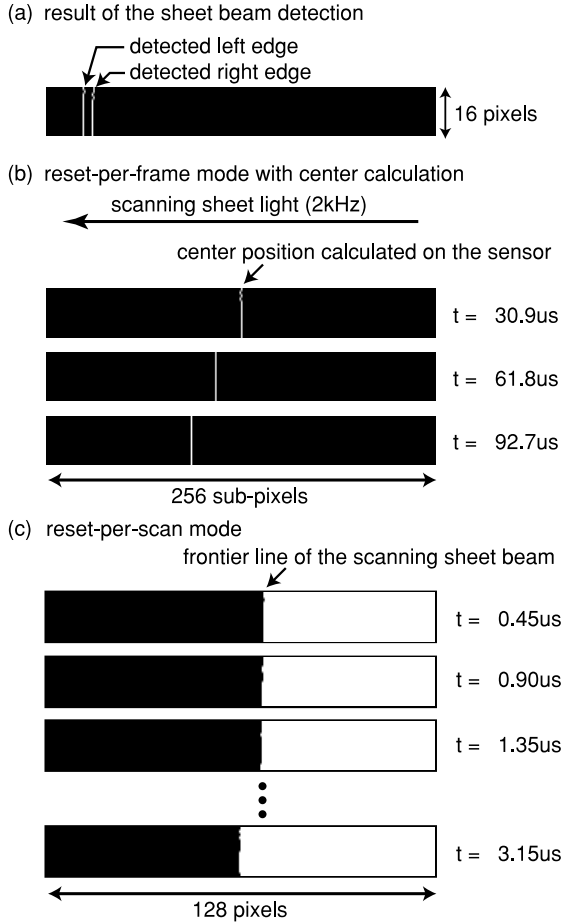
tion. Therefore the frame rate f_{psd} could be limited by the pixel-activation rate f_{pa1} if the intensity of projected beam is insufficient. The pixel-activation rate of a reset-per-scan mode can be ~ 233 kHz in our measurement system, where the efficiency Q of Eq. (17) is about $1/7$. That is, the possible frame rate f_{psd} of the system with 128-pixel horizontal resolution is 233k fps limited by the intensity of projected beam. On the other hand, the measurement results also show that our position sensor achieves $f_{psd} = 2.22$M fps if we have an acceptable test equipment with a plenty strong projected beam and a higher-speed scanning mirror. To achieve the maximum frame rate in the present sensor, we need a high-power laser beam source with 2.5 W. It can be reduced by using a high-sensitive photo detector instead of the current photo detector in a standard digital CMOS process.

Its performance and comparisons are summarized in Table 2. The sensors [6], [8] are the state-of-the-art high-speed range finders based on a light-section method. [8] has 320×240 pixel resolution for color 2-D imaging though only 160×120 pixels are effective for range finding. Our position detector achieves high-speed position detection to realize beyond-real-time range finding and it has a possibility of high frame rate in a large pixel array.

7. Conclusions

A row-parallel sensor architecture and its circuit implementation have been proposed for a high-speed 3-D camera using a light-section method. In our search architecture, the positions of activated pixels are quickly detected by a row-parallel search circuit in pixel and a row-parallel address acquisition of $O(\log N)$ cycles in N-pixel horizontal resolution. The architecture has a possibility of high-speed position detection in high pixel resolution and we have shown its applicability to a large pixel array by simulation. The prototype position sensor with 128×16 pixels has been designed and fabricated in $0.35\,\mu$m CMOS process and successfully tested. In the measurement system using an FPGA at 80 MHz operation, it achieves quick activated-position

Fig. 16 Measurement results.

Table 2 Measurement results and comparisons.

	# pixels	frame rate	range_map/sec (rps)	limiting factor
Our position detector	128×16	32.2k fps[1]	252 rps	f_{pa}: activation rate
– reset per frame	1024×1024	(31.4k fps)[2]	30.6 rps	f_{acc}: access rate
Our position detector	128×16	233k fps[1]	1.74k rps[3]	f_{pa}: activation rate
– reset per scan	128×16	2.22M fps[1]	17.3k rps[4]	f_{acc}: access rate
	1024×1024	(1.09M fps)[2]	1.06k rps	f_{acc}: access rate
Brajovic et al. [6]	32×64	6.4k fps	100 rps	f_{acc}: access rate
Sugiyama et al. [8]	160×120	3.3k fps	15 rps	f_{acc}: access rate
Required fps for real time	1024×1024	30.7k fps	(for 30 rps)	—

[1] Meaurement results with 2 kHz scanning beam of 300 mW.
[2] Simulation results in parentheses.
[3] Possible range finding rate with high-speed scanning mirror.
[4] Possible range finding rate with strong beam intensity.

detection of 450 ns in row parallel. The access rate of activated pixels achieves 2.22 MHz. We have discussed on the limiting factors of frame rate and shown 32.2k-fps and 233k-fps position detection with 2 kHz scanning beam of 300 mW in a reset-per-frame mode and a reset-per-scan mode respectively. The measurement results also show that the maximum frame rate is limited by the access rate of 2.22M fps if a sufficient light is available. It has the capability of quick position detection to realize a high-speed 3-D camera for "beyond-real-time" range finding and visual feedback.

Acknowledgment

References

[1] A. Krymski, D.V. Blerkom, A. Andersson, N. Bock, B. Mansoorian, and E.R. Fossum, "A high speed, 500 frames/s, 1024 × 1024 CMOS active pixel sensor," IEEE Symp. VLSI Circuits Dig. of Tech. Papers, pp.137–138, 1999.

[2] S. Kleinfelder, S. Lim, X. Liu, and A.E. Gamal, "A 10k frame/s 0.18 μm CMOS digital pixel sensor with pixel-level memory," IEEE Int. Solid-State Circuits Conf. (ISSCC) Dig. of Tech. Papers, pp.88–89, 2001.

[3] V. Brajovic and T. Kanade, "Computational sensor for visual tracking with attention," IEEE J. Solid-State Circuits, vol.33, no.8, pp.1199–1207, Aug. 1998.

[4] T. Nezuka, M. Hoshino, M. Ikeda, and K. Asada, "A position detection sensor for 3-D measurement," Proc. European Solid-State Circuits Conference (ESSCIRC), pp.412–415, 2000.

[5] M. de Bakker, P.W. Verbeek, E. Nieuwkoop, and G.K. Steenvoorden, "A smart range image sensor," Proc. European Solid-State Circuits Conference (ESSCIRC), pp.208–211, 1998.

[6] V. Brajovic, K. Mori, and N. Jankovic, "100 frames/s CMOS range image sensor," IEEE Int. Solid-State Circuits Conf. (ISSCC) Dig. of Tech. Papers, pp.256–257, 2001.

[7] S. Yoshimura, T. Sugiyama, K. Yonemoto, and K. Ueda, "A 48k frame/s CMOS image sensor for real-time 3-D sensing and motion detection," IEEE Int. Solid-State Circuits Conf. (ISSCC) Dig. of Tech. Papers, pp.94–95, 2001.

[8] T. Sugiyama, S. Yoshimura, R. Suzuki, and H. Sumi, "A 1/4-inch QVGA color imaging and 3-D sensing CMOS sensor with analog frame memory," IEEE Int. Solid-State Circuits Conf. (ISSCC) Dig. of Tech. Papers, pp.434–435, 2002.

Yusuke Oike was born in Tokyo, Japan on July 4th, 1977. He received the B.S. and M.S. degree in electronic engineering from University of Tokyo, Tokyo, Japan, in 2000 and 2002, respectively. Presently, he is working towards the Ph.D. degree in the Department of Electronic Engineering of University of Tokyo. His current research interests include architecture and design of smart image sensors, mixed-signal circuits and functional memories. He has received the best design award from IEEE Int. Conf. VLSI Design & ASP-DAC. He is a student member of The Institute of Electrical and Electronics Engineers (IEEE), and The Institute of Image Information and Television Engineers (ITE).

Makoto Ikeda received the B.S., M.S., and Ph.D. in electronics engineering from the University of Tokyo, Tokyo, Japan, in 1991, 1993, and 1996, respectively. He joined EE department of University of Tokyo as a faculty member in 1996, and is currently an associate professor at VLSI Design and Education Center, University of Tokyo. His interests are in architecture and design of content addressed memories and its applications. He is a member of Institute of Electrical and Electronics Engineers (IEEE) and Information Processing Society of Japan (IPSJ).

Kunihiro Asada was born in Fukui, Japan, on June 16th, 1952. He received the B.S., M.S., and Ph.D. in electronic engineering from University of Tokyo in 1975, 1977, and 1980, respectively. In 1980 he joined the Faculty of Engineering, University of Tokyo, and became a lecturer, an associate professor and a professor in 1981, 1985 and 1995, respectively. From 1985 to 1986 he stayed in Edinburgh University as a visiting scholar supported by the British Council. From 1990 to 1992 he served as the first Editor of English version of IEICE (Institute of Electronics, Information and Communication Engineers of Japan) Transactions on Electronics. In 1996 he established VDEC (VLSI Design and Education Center) with his colleagues in University of Tokyo. It is a center supported by the Government to promote education and research of VLSI design in all the universities and colleges in Japan. He is currently in charge of the head of VDEC. His research interest is design and evaluation of integrated systems and component devices. He has published more than 390 technical papers in journals and conference proceedings. He has received best paper awards from IEEJ (Institute of Electrical Engineers of Japan), IEICE and ICMTS1998/IEEE and so on. He is a member of IEEE and IEEJ. He is currently Chair of IEEE/SSCS Japan Chapter.